IJC
International Journal of Cancer

The GEF-H1/PKD3 signaling pathway promotes the maintenance of triple-negative breast cancer stem cells

Wolfgang S. Lieb[1], Cristiana Lungu[1], Raluca Tamas[1], Hannah Berreth[1], Philipp Rathert[2], Peter Storz[3], Monilola A. Olayioye[1] and Angelika Hausser[1]

[1]Institute of Cell Biology and Immunology and Stuttgart Research Center Systems Biology, University of Stuttgart, Stuttgart, Germany
[2]Biochemistry Department, Institute of Biochemistry and Technical Biochemistry, University of Stuttgart, Stuttgart, Germany
[3]Department of Cancer Biology, Mayo Clinic, Jacksonville, FL

Protein kinase D3 (PKD3) is upregulated in triple-negative breast cancer (TNBC) and associated with cell proliferation and metastasis development but its precise pro-oncogenic function is unknown. Here we show that PKD3 is required for the maintenance of the TNBC stem cell population. The depletion of PKD3 in MDA-MB-231 cells reduced the cancer stem cell frequency *in vitro* and tumor initiation potential *in vivo*. We further provide evidence that the RhoGEF GEF-H1 is upstream of PKD3 activation in TNBC stem cells. Most importantly, pharmacological PKD inhibition in combination with paclitaxel synergistically decreased oncosphere and colony formation efficiency *in vitro* and tumor recurrence *in vivo*. Based on our results we propose that targeting the GEF-H1/PKD3 signaling pathway in combination with chemotherapy might provide an effective therapeutic option for TNBC.

Introduction

Despite improved early detection and the development of novel therapeutics, triple-negative breast cancer (TNBC) still is associated with a high mortality rate. TNBC accounts for 15–20% of all breast carcinomas and is characterized by the lack of estrogen and progesterone receptors (ER/PR) and HER2 overexpression.[1] Compared to HER2 and ER/PR positive breast cancers TNBC is associated with an increased risk for metastasis and lower 5-year survival.[2–4] TNBC treatment is mainly based on chemotherapeutics such as anthracyclines and taxanes, however, many TNBCs rapidly develop resistance to these drugs.[5] Notably, after the treatment with taxanes an expansion of $CD44^+/CD24^-$ and aldehyde dehydrogenase 1 (ALDH)-positive TNBC cells was observed.[6–8] Expression of these markers is characteristic of cancer stem cells (CSC), a small subpopulation of undifferentiated cells within the tumor mass. The presence of CSC is linked to early metastases, faster tumor recurrence and worse overall survival.[9–12] Moreover, apart from infinite proliferation and self-renewal, CSCs have the capability to initiate tumor formation.[13] Understanding the mechanisms that underlie the self-renewal behavior and survival of CSCs is thus critical for developing novel therapeutic strategies that also target CSCs.

The protein kinase D (PKD) family comprising PKD1, PKD2 and PKD3 is best known for controlling vesicle fission at the Golgi complex and actin remodeling during cell migration (reviewed in Refs. 14 and 15). In normal breast tissue, PKD1 is the predominant isoform but its gene expression is suppressed during cancer progression by epigenetic silencing.[16] In TNBC, an isoform switch toward high PKD3 expression occurs, resulting from the lack of ER, a repressor of PKD3 gene expression.[17,18] Elevated PKD3 levels are associated with increased proliferation and cell motility, metastatic progression, as well as poor prognosis, supporting a pro-oncogenic role for PKD3 in TNBC.[17,19,20] However, molecular pathways controlling the activity of PKD3 and its precise pro-oncogenic function in TNBC have remained elusive.

By targeted cell surface screening, we have discovered a novel function for PKD3 in the maintenance of CSCs. We show that the loss of PKD3 in TNBC cell lines reduced the stem cell frequency *in vitro* and decreased the tumor initiation potential of implanted MDA-MB-231 cells *in vivo*. We further provide evidence that the function of PKD3 in the maintenance of CSCs requires upstream activation by the Rho guanine nucleotide exchange factor 2 (GEF-H1). Significantly, the combinatorial treatment with the pharmacological PKD

Additional Supporting Information may be found in the online version of this article.
Key words: cancer stem cells, TNBC, PKD3, paclitaxel, ALDH
Conflict of interest: The authors have no conflict of interest to declare.
Grant sponsor: Deutsche Krebshilfe; **Grant number:** 70111941;
Grant sponsor: NIH; **Grant numbers:** CA184527, CA200572

DOI: 10.1002/ijc.32798
History: Received 15 Jul 2019; Accepted 14 Nov 2019; Online 14 Dec 2019
Correspondence to: Angelika Hausser, E-mail: angelika.hausser@izi.uni-stuttgart.de; or Monilola A. Olayioye, E-mail: monilola.olayioye@izi.uni-stuttgart.de

What's new?

The serine-threonine kinase PKD3 is upregulated in triple-negative breast cancer (TNBC) and associated with cell proliferation and metastasis. The mechanisms underlying PKD3 pro-oncogenic function remain unclear, however. Here, the authors reveal a critical role for PKD3 in the maintenance and propagation of TNBC stem cells *in vitro* and *in vivo*. The function of PKD3 in the maintenance of cancer stem cells requires upstream activation by GEF-H1. Importantly, the PKD inhibitor CRT0066101 and paclitaxel synergistically decrease TNBC stem cell prevalence and tumor recurrence *in vivo*. The results provide a rationale for targeting PKD3 to eliminate the tumor-initiating cell population in TNBC.

inhibitor CRT0066101 and the chemotherapeutic paclitaxel was superior in reducing oncosphere formation *in vitro* and tumor recurrence *in vivo* when compared to monotherapy. Our results thus demonstrate the importance of PKD3-mediated CSC regulation and provide a rationale for targeting the GEF-H1/PKD3 signaling pathway to eliminate the tumor-initiating cell population in TNBC.

Materials and Methods

Cell culture and cell line authentication

MDA-MB-231 cells (CLS, RRID:CVCL_0062) and MDA-MB-231-based knockdown cell lines (shNon_CTRL, shPKD3_1, shPKD3_2[17]) were cultured in DMEM low glucose. MDA-MB-436 cells (Dr. Margarete Fischer-Bosch Institute of Clinical Pharmacology, Stuttgart, RRID:CVCL_0623) were cultured in DMEM high glucose. MDA-MB-468 (CLS, RRID:CVCL_0419), BT-549 (CLS, RRID:CVCL_1092), HCC1806 (ATCC, RRID: CVCL_1258), SKBR3 (CLS, RRID:CVCL_0033), T47D (Dr. Margarete Fischer-Bosch Institute of Clinical Pharmacology, Stuttgart, RRID:CVCL_055) and MCF7 (Dr. Margarete Fischer-Bosch Institute of Clinical Pharmacology, Stuttgart, RRID: CVCL_0031) cells were cultured in RPMI-1640. All media were supplemented with 10% fetal bovine serum (PAA Laboratories, Waltham, MA). MCF10A_EcoR_PKD3WT-EGFP (generated in our study) and MCF10A cells (Department of Biomedicine, University of Basel, RRID:CVCL_0598) were cultured in DMEM/F12 GlutaMAX supplemented with 5% horse serum, 20 ng/ml EGF, 0.5 μg/ml hydrocortisone, 100 ng/ml cholera toxin and 10 μg/ml insulin. All cell lines were cultured at 37°C in a humidified chamber with 5% CO_2, tested negative for *Mycoplasma* (Lonza, LT07-318) and were authenticated within the last 3 years by SNP profiling (Multiplexion GmbH).

Cell surface protein screen

LEGENDScreen kit was used according to the manufacturer's instructions. In brief, cells were detached with accutase and seeded (3×10^4 cells) into 96-well plates containing the prediluted PE-labeled antibodies. After 40 min of incubation at 4°C, cells were fixed for 10 min at RT, washed and analyzed by flow cytometry using MACSQuant® Analyzer 10 (Miltenyi Biotec, Bergisch Gladbach, Germany). Data were evaluated using FlowJo. Relative mean fluorescence intensities (rel. MFI) were calculated as follows: rel. MFI = $[MFI_{sample} - (MFI_{isotype} - MFI_{cells})]/MFI_{cells}$. Rel MFI values <1.5 were not considered. After normalizing to shNon_CTRL, surface proteins in the shPKD3_1 cells with values ≤0.9 were considered to be downregulated, those with values ≥1.1 were considered to be upregulated.

Sphere formation assays

For extreme limiting dilution assays (ELDA), cells were trypsinized, singularized using a 27G needle and 1, 10 or 100 cells were seeded onto Poly(2-hydroxyethyl methacrylate)-(pHEMA)-treated 96-well plates, respectively. Cells were cultured in 300 μl sphere formation medium containing DMEM/F12 GlutaMAX supplemented with 10 μg/ml insulin, 20 ng/ml EGF, 1 μg/ml hydrocortisone and 1x B27-supplement. Twenty technical replicates per condition were cultured for 10 days. Only wells positive for spheres, no matter the actual number, were regarded as a positive. Multiple group comparison and estimated stem cell frequency were analyzed using the ELDA software.[21]

For primary sphere formation assays, cells were trypsinized, singularized using a 27G needle, seeded onto pHEMA-treated plates in sphere formation medium and cultured for 5 days. For secondary sphere formation assays, primary spheres were collected, trypsinized, singularized and cultured as described above. shNon, shPKD3_1, shPKD3_2, MDA-MB-231, MDA-MB-468, MDA-MB-436, HCC1806 and MCF7 cells were seeded onto 12-well plates (primary assay: 3×10^3 cells; secondary assay: 1×10^3 cells) in 1.5 ml sphere formation medium. BT-549 cells were seeded onto six-well plates (primary/ secondary assay: 5×10^3 cells) in 3 ml sphere formation medium. MCF10A_ EcoR_PKD3WT-EGFP cells were pretreated with doxycycline (Dox) for 24 hr before the cells were singularized and seeded (5×10^3 cells) onto six-well plates in 3 ml sphere formation medium. Subsequently, the sphere formation medium was supplemented with Dox and cells were cultured for 5 days. Spheres were imaged and the sphere area was analyzed using ImageJ. Only spheres larger than 2,500 μm^2 were taken into consideration. Data are presented as sphere area (mm^2) or sphere formation efficiency (SFE; spheres formed per 1,000 cells seeded).

ALDH activity assay

For the ALDH assay, 1×10^5 singularized cells were diluted in 100 μl Assay Buffer containing 1.5 μl of activated ALDEFLUOR Reagent. Subsequently, 50 μl were removed and mixed with 1.5 μl DEAB Reagent (control). Control and test samples were incubated at 37°C for 30 min, followed by flow cytometry analysis using MACSQuant Analyzer 10 (Miltenyi Biotec). Data were evaluated using FlowJo. DEAB treated samples served as internal controls.

Orthotopic tumor models

Animal experiments were approved by state authorities and carried out according to federal guidelines. For the ELDA, 8-week-old female SCID mice were injected with 5×10^5 or 5×10^4 MDA-MB-231 shNon_CTRL or shPKD3_1 cells in 100 µl PBS into the right fat pad of the 4th nipple. Tumor growth was analyzed by caliper measurements. Mice were sacrificed after 8 weeks. Multiple group comparisons and estimated stem cell frequency were analyzed using the ELDA software.[21] Tumors were imaged, dissociated according to the manufacturer's instructions and processed for oncosphere formation assays and ALDH analysis.

For combined paclitaxel and CRT0066101 treatment, 8-week-old female SCID mice were injected with 2×10^6 MDA-MB-231 cells in 100 µl PBS into the right fat pad of the 4th nipple. Tumor growth was analyzed by caliper measurements ((length × width^2)/2). After the tumors had reached 100 mm^3 mice were assigned to control and three treatment groups ($n = 7$ mice per group). During the following treatment-phase (21 days), mice were treated with either (*i*) CRT0066101 (peroral, 80 mg/kg diluted in a 5% dextrose saline solution), (*ii*) paclitaxel (intraperitoneal injection, 10 mg/kg body weight diluted in a 10% polysorbate PBS solution), (*iii*) CRT0066101 in combination with paclitaxel or (*iv*) the combination of the respective carriers (control). Paclitaxel was injected on Day 23, 30, 37 and 44. CRT0066101 was given once daily from Day 23 to Day 43. After the treatment-phase, tumor growth was monitored for 20 additional days.

Statistical analysis

Data are presented as mean ± SEM. Significance between multiple groups was determined by one-way or two-way ANOVA and Bonferroni's test for multiple comparison. Significance between the two groups was determined by *t*-test. Data were analyzed using GraphPad Prism 7. *p* values: $p \leq 0.05$ (*), $p \leq 0.01$ (**), $p \leq 0.001$ (***), $p \leq 0.0001$ (****). Combination index (CI) values were calculated using Webb's fractional product method. CI < 1 indicates synergism, $1 \leq CI \leq 1.09$ addition and CI > 1.09 antagonism.

Additional material and methods can be found in the Supporting Information Materials and Methods.

Data availability

The data that support the findings of our study are available from the corresponding author upon reasonable request.

Results

PKD3 depletion decreases CSC-like properties in MDA-MB-231 cells

It is well established that PKD3 controls vesicular traffic to the plasma membrane thereby modulating the expression of cell surface proteins.[22] To analyze how PKD3 controls the cell surface phenotype of breast cancer cells, we used the TNBC cell line MDA-MB-231 stably depleted of PKD3 (shPKD3_1)[17] and performed a flow cytometry-based screening of 332 molecules (Fig. 1*a*). MDA-MB-231 cells stably expressing a scrambled shRNA were used as control (shNon_CTRL; Supporting Information Figs. S1*a* and S1*b*). About 102 cell surfaces proteins were above the detection threshold (Supporting Information Table S1). In the PKD3 deficient cells, 68 proteins displayed dysregulated surface levels with respect to the control (24 upregulated and 44 downregulated). Several of the proteins with decreased cell surface expression have been associated with the maintenance of breast CSCs, such as CD44, CD184, CD61, NOTCH2, NOTCH4 and CD304[6,7,23–27] (Fig. 1*b*, Supporting Information Figs. S1*c*–S1*h*, Table S1). This prompted us to measure the stem cell frequency of the stable MDA-MB-231 cell lines by performing extreme limiting dilution assays (ELDA; Fig. 1*c*). Indeed, the estimated stem cell frequency was significantly decreased in PKD3 depleted cells when compared to the stem cell frequency of the control cells (Fig. 1*d*). We then analyzed the gene expression of a panel of breast cancer stemness markers including SOX2, OCT3/4, NANOG, NOTCH4, CD44, SNAI1 and ALDH1 in monolayer (2D)-cultured shPKD3_1 and shNon_CTRL cells.[11,28] Compared to the control cells, we observed a significant downregulation of the corresponding genes in shPKD3_1 cells (Fig. 1*e*). Enhanced ALDH activity is considered a hallmark of breast CSCs.[29,30] When comparing MDA-MB-231 shPKD3_1 cells with shNon_CTRL cells, we observed that PKD3 depletion caused a significant decrease in ALDH activity as measured by aldefluor assay (Fig. 1*f*), which further substantiated a potential role of the kinase in stem cell regulation. Finally, we investigated the formation of primary and secondary oncospheres as a measure of CSC activity.[31] Here, the depletion of PKD3 caused an up to 70% decrease in primary and secondary sphere-forming efficiency (SFE) (Fig. 1*g*) in comparison to the control. Remarkably, the knockdown of PKD3 neither changed the size of the oncospheres (Fig. 1*h*), nor did it induce cell death by anoikis, excluding antiproliferative and proapoptotic effects (Supporting Information Figs. S1*i* and S1*j*).

In an independent MDA-MB-231 PKD3 knockdown cell line, shPKD3_2,[17] we could confirm the significant downregulation of stemness-related marker gene expression (Supporting Information Fig. S1*k*), ALDH activity (Supporting Information Fig. S1*l*) and oncosphere forming efficiency (Supporting Information Figs. S1*m* and S1*n*) upon loss of PKD3 expression. Activation of YAP (yes-associated protein)/YAZ (transcriptional co-activator with PDZ-binding motif) and Notch signaling are required to sustain self-renewal and tumor-initiation capacities in breast CSCs.[27,32] Indeed, in both PKD3 knockdown cell lines, decreased expression of the YAP/TAZ and Notch target genes CTGF and HES1/HEY1, respectively, indicated impaired signaling through these pathways (Supporting Information Fig. S1*o*). We further observed downregulation of ABCG2, which contributes to drug resistance in breast CSCs (Supporting Information Fig. S1*o*)[8] and the *bona fide* EMT marker gene SLUG (Supporting Information Fig. S1*o*). These results were confirmed in BT549 cells in which the depletion of PKD3 significantly increased CDH1 levels while

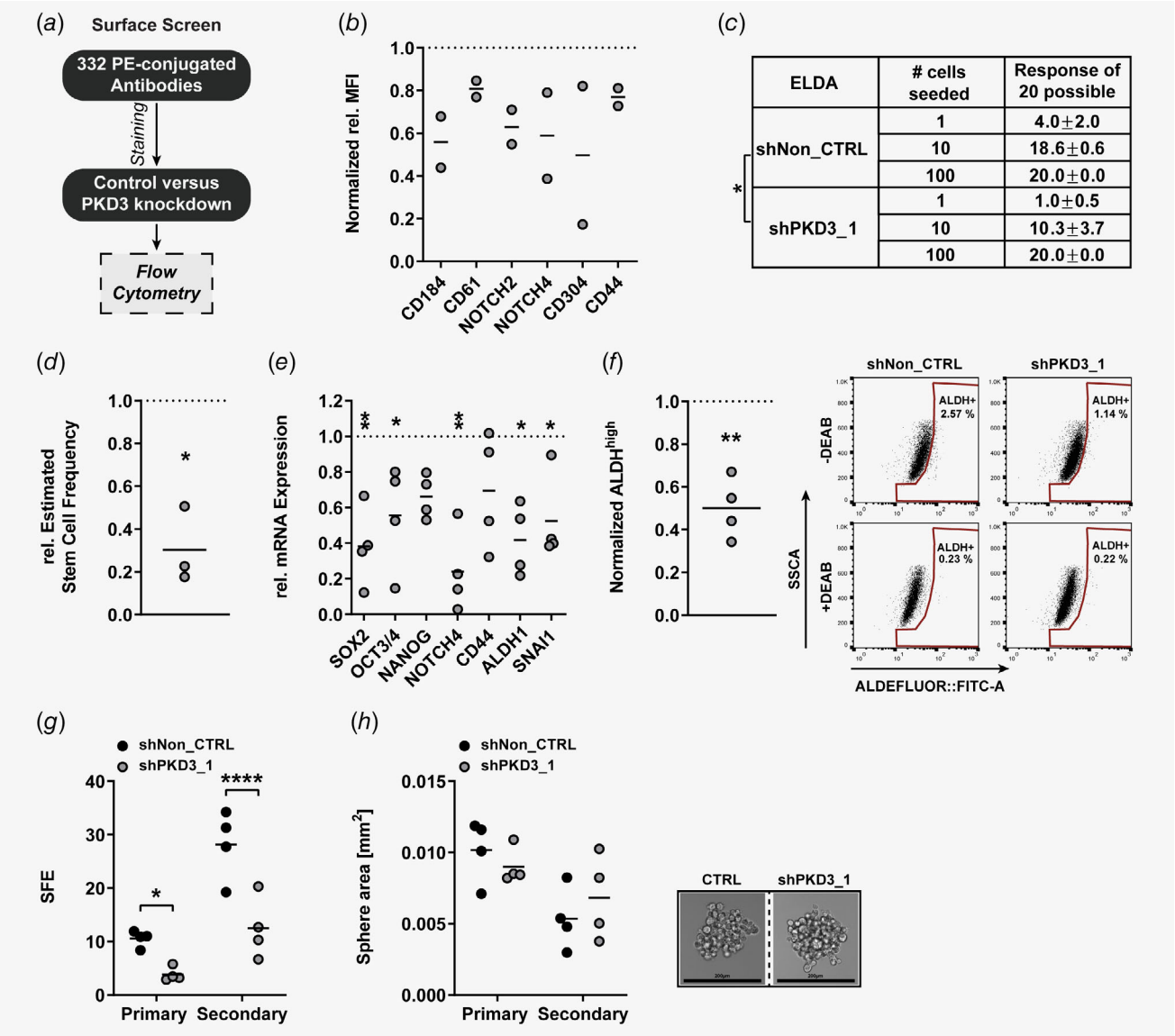

Figure 1. Loss of PKD3 reduces stemness in MDA-MB-231 cells. (*a*) Cell surface screen workflow. (*b*) Flow cytometry-based surface protein screening. Data are presented as relative mean fluorescence intensity (rel. MFI) normalized to shNon_CTRL, $n = 2$. (*c*) ELDA, analysis of 20 wells of a 96-well plate per condition. Only sphere-positive wells were considered. Data are presented as mean ± SEM, $n = 3$. Statistical comparison by ELDA multiple group analysis. (*d*) ELDA-based estimated stem cell frequency. Data are presented as mean estimated stem cell frequency normalized to shNon_CTRL, $n = 3$. Statistical comparison by *t*-test. (*e*) qPCR analysis of stemness markers. Data are presented as mean mRNA expression normalized to shNon_CTRL, $n = 4$. Statistical comparison by *t*-test. (*f*) *Left*: flow cytometry-based ALDH activity analysis. Data are presented as mean $ALDH^{high}$ population normalized to shNon_CTRL, $n = 4$. Statistical comparison by *t*-test. *Right*: Dot plot of ALDH measurements. (*g*) Mean SFE of primary and secondary oncosphere assays, $n = 4$. Statistical comparison by one-way ANOVA and Bonferroni test. (*h*) *Left*: mean sphere area of primary and secondary oncospheres, $n = 4$. *Right*: representative oncosphere pictures. Scale bar: 200 µm. [Color figure can be viewed at wileyonlinelibrary.com]

SNAI1 and SLUG levels were reduced (Supporting Information Fig. S1*p*). Thus, our results univocally show that MDA-MB-231 cells require PKD3 for CSC maintenance *in vitro*.

PKD3 knockdown decreases the tumor initiation potential *in vivo*

To prove that PKD3 is also important for maintaining the tumor initiation potential *in vivo*, we implanted four different concentrations of MDA-MB-231 shPKD3_1 and shNon_CTRL cells into the fourth mammary fat pad of immunocompromised mice (Fig. 2*a*). Strikingly, shPKD3_1 Cells exhibited a strongly diminished tumor initiation potential compared to shNon_CTRL cells (Figs. 2*b* and 2*c*). In line with the reduced tumor initiation potential, the estimated stem cell frequency of PKD3 deficient tumor cells was significantly lower (Fig. 2*c*). Apart from the lowest cell concentration injected, shNon_CTRL and shPKD3_1 tumors did not differ in size (Fig. 2*d*). We next singularized the tumor cells, analyzed ALDH activity (Fig. 2*e*) and

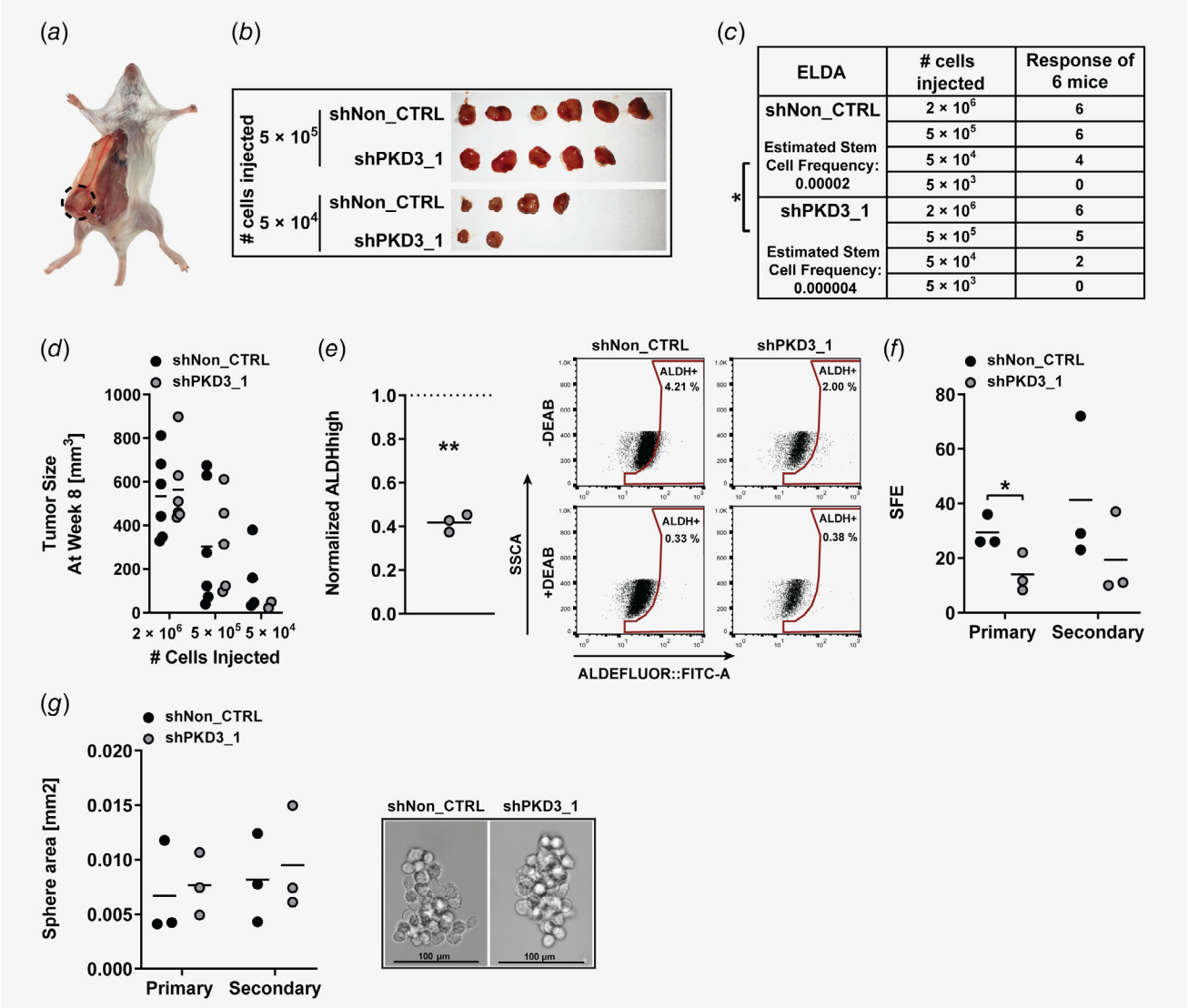

Figure 2. *In vivo* tumor initiation potential is decreased in PKD3-depleted TNBC cells. (*a*) Representative picture of orthotopic tumor formation. (*b*) Tumors of mice injected with 5×10^5 and 5×10^4 MDA-MB-231 cells expressing the indicated shRNAs. (*c*) ELDA, six mice per condition. Data are presented as tumor-bearing mice per injected cell concentration and estimated stem cell frequency. Statistical comparison by ELDA multiple group analysis. (*d*) Tumor size at Week 8, $n = 2–6$. Statistical comparison by one-way ANOVA and Bonferroni-test. (*e*) *Left*: flow cytometry-based ALDH activity analysis of singularized tumor cells. Data are presented as mean $ALDH^{high}$ population of shPKD3_1 normalized to shNon_CTRL, $n = 3$. Statistical comparison by *t*-test. *Right*: Dot plot of ALDH measurements. (*f*) Mean SFE of primary and secondary oncosphere assays, $n = 3$. Statistical comparison by *t*-test. (*g*) *Left*: mean sphere area of primary and secondary oncospheres, $n = 3$. *Right*: representative oncosphere pictures. Scale bar: 100 µm.

primary as well as secondary oncosphere formation (Figs. 2*f* and 2*g*). In agreement with the decreased stem cell frequency, ALDH activity and SFE were significantly reduced in PKD3 deficient MDA-MB-231 tumor cells. Our data thus confirm a role for PKD3 in promoting stemness and tumor-initiating capacity of MDA-MB-231 cells.

PKD3-mediated TNBC stem cell regulation is dependent on GEF-H1

We recently reported that GEF-H1 is an upstream activator of PKD at the Golgi complex in HeLa cells[33] (Fig. 3*a*). Therefore, we analyzed whether GEF-H1 is required for PKD3 to promote TNBC cell stemness. To drive Rho-dependent PKD activation we treated MDA-MB-231 cells with nocodazole[33] and detected PKD activity by activation loop phosphorylation (pS744/748), which is conserved in all PKD isoforms. Treatment with PMA, a potent inducer of PKD activity,[14] served as a positive control. Nocodazole strongly increased PKD activity and this was fully abrogated by PKD3 depletion despite the presence of PKD2. Importantly, nocodazole failed to induce PKD activity in the absence of GEF-H1, proving that PKD3, but not PKD2, is activated by GEF-H1 in MDA-MB-231 cells (Fig. 3*b*).

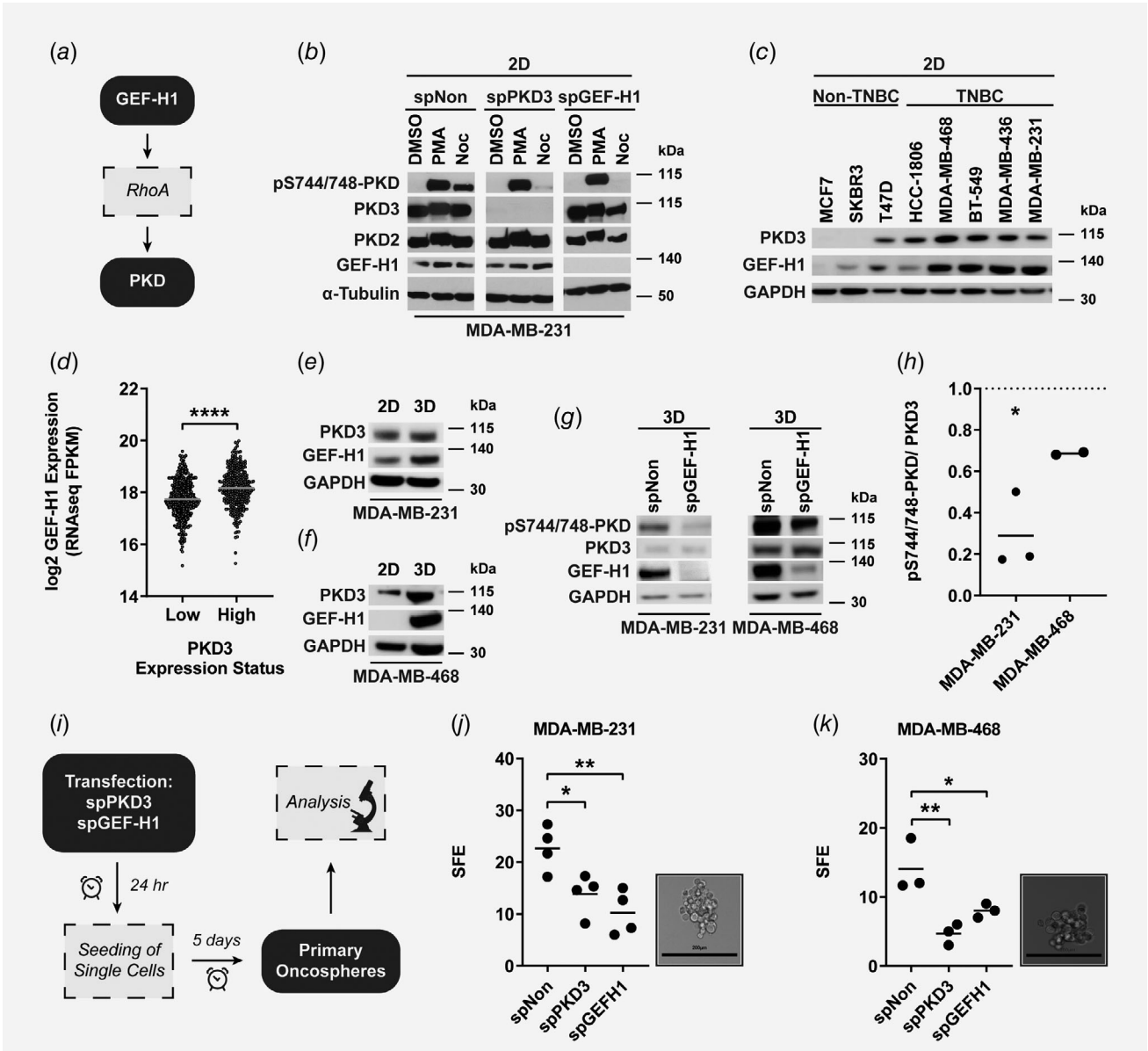

Figure 3. GEF-H1-mediated activation of PKD3 is crucial for mammosphere formation. (*a*) Scheme showing the GEF-H1/PKD3 signaling pathway. (*b*) Western blot of MDA-MB-231 cells treated with nocodazole (Noc; 5 μg/ml, 1 hr), phorbol 12-myristate 13-acetate (PMA; 1 μM, 15 min) or DMSO. Before treatment, MDA-MB-231 cells were transiently transfected with smartpool (sp) siRNAs as indicated. Membranes were probed with specific antibodies as indicated. α-tubulin was used as loading control. *(c)* Western blot of TNBC and non-TNBC cell lines. Membranes were probed with specific antibodies as indicated. GAPDH was used as loading control. (*d*) GEF-H1 mRNA expression levels within PKD3 high and low expression groups in tumor samples from the TCGA-BRCA project. The samples were divided according to PKD3 expression by tertile separation, where "PKD3 low" is represented by the lower tertile (quantile ‹0.33, $n = 403$) and "PKD3 high" by the upper tertile (quantile ›0.67, $n = 312$), normal tissue samples excluded. GEF-H1 expression is visualized as log2[GEF-H1 expression (FPKM) + 0.01]. (*e*, *f*) Western blot of *(e)* MDA-MB-231 and (*f*) MDA-MB-468 cells, comparing monolayer-cultured cells (2D) with oncospheres (3D). Immunoblotting was conducted, and membranes were probed with specific antibodies as indicated. GAPDH was used as loading control. (*g*) Western blot of MDA-MB-231 and MDA-MB-468 oncospheres. 24 hr prior to seeding, MDA-MB-231 and MDA-MB-468 cells were transiently transfected with smartpool (sp) siRNAs as indicated. Membranes were probed with specific antibodies as indicated. GAPDH was used as loading control. (*h*) Quantification of data shown in (*g*), using densitometry analysis. Data are presented as mean line density of spGEF-H1 normalized to spNon, $n = 2–3$. Statistical comparison by *t*-test. (*i*) Workflow: Oncosphere formation assay of transfected cells. (*j*,*k*) *Left*: Mean SFE of primary oncosphere assays of (*j*) MDA-MB-231 and (*k*) MDA-MB-468 cells. Then, 24 hr prior to seeding, MDA-MB-231 and MDA-MB-468 cells were transiently transfected with smartpool (sp) siRNAs as indicated, $n = 3–4$. Statistical comparison by one-way ANOVA and Bonferroni test. *Right*: representative oncosphere pictures. Scale bar: 200 μm.

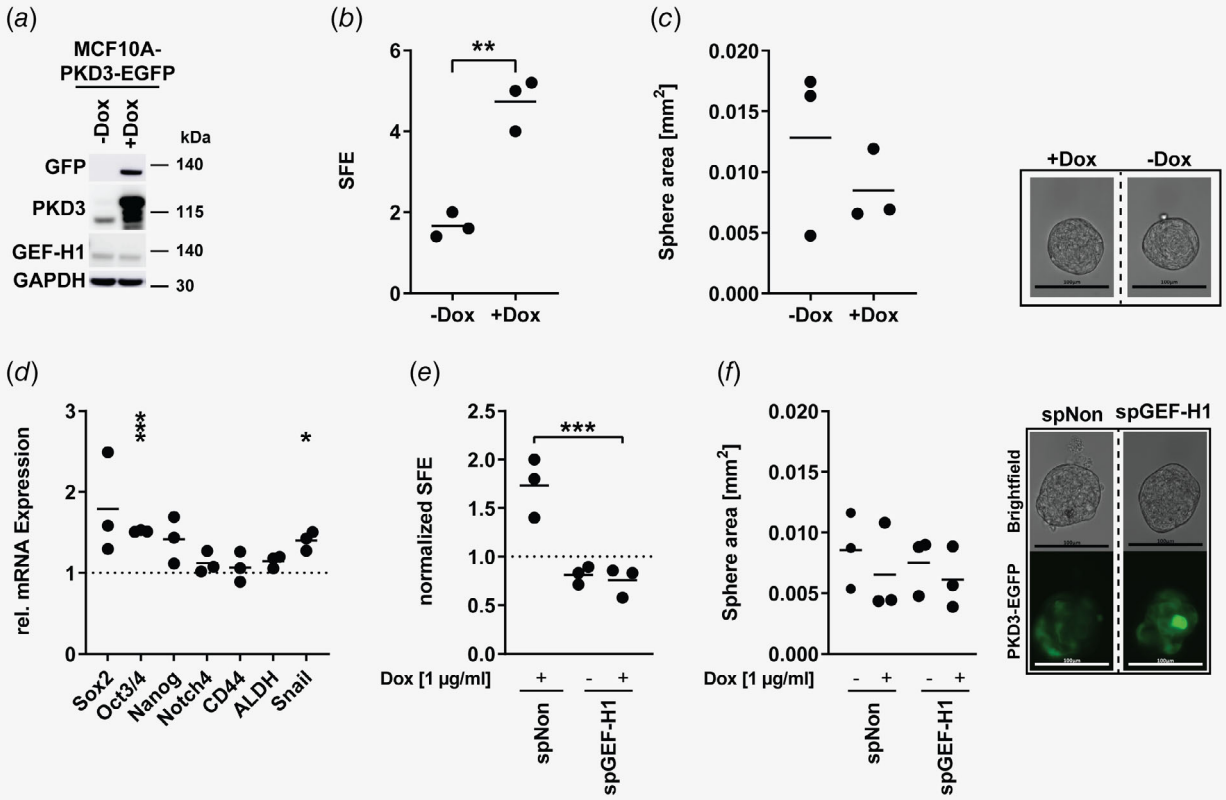

Figure 4. PKD3 overexpression-induced sphere formation is dependent on GEF-H1. (*a*) Western blot of MCF10A-EcoR-PKD3WT cells. Cells were treated with doxycycline (+Dox) for 48 hr. Water served as control (−Dox). Membranes were probed with specific antibodies as indicated. GAPDH was used as loading control. (*b*) Mean SFE of primary oncosphere formation assays of MCF10A-EcoR-PKD3WT-EGFP cells. Then, 24 hr prior to and directly after seeding cells into the oncosphere assay the medium was supplemented with Dox and spheres were grown for 5 days, $n = 3$. Statistical comparison by *t*-test. (*c*) *Left*: mean sphere area of primary oncospheres, $n = 3$. Statistical comparison by *t*-test. *Right*: representative oncosphere pictures. Bar represents 100 µm. (*d*) qPCR analysis of stemness markers. Data are presented as mean mRNA expression of Dox-treated cells normalized to untreated control, $n = 3$. Statistical comparison by *t*-test. (*e*–*f*) 48 hr prior to seeding MCF10A-EcoR-PKD3WT-EGFP cells were transiently transfected with smartpool (sp) siRNAs as indicated. Then, 24 hr prior to and directly after seeding into the oncosphere assay, cells were treated with Dox. (*e*) Mean SFE of primary oncosphere assay. Data were normalized to untreated spNon, $n = 3$. Statistical comparison by one-way ANOVA and Bonferroni test. (*f*) *Left*: *mean* sphere area of primary spheres, $n = 3$. *Right*: representative pictures of transiently transfected and Dox-treated (continuously for 6 days) MCF10A-PKD3-EGFP cells after 5 days in the oncosphere formation assay. Scale bar: 100 µm.

We next analyzed the correlation of GEF-H1 and PKD3 expression in a panel of breast cancer cell lines. In general, TNBC cell lines with elevated PKD3 expression[19] also expressed higher GEF-H1 levels whereas low PKD3 and GEF-H1 expression were observed in the non-TNBC cell lines (Fig. 3*c*). To verify these findings in clinical patient data, we analyzed PKD3 and GEF-H1 mRNA levels in human breast cancers from the TCGA database. In accordance with the cell line data, significantly higher GEF-H1 expression was observed in the tumor samples belonging to the high PKD3 expression group (Fig. 3*d*). We next addressed the functional relevance of GEF-H1 and PKD3 expression in primary oncospheres (3D) obtained from two independent TNBC cell lines (Figs. 3*e* and 3*f*). In both MDA-MB-231 and MDA-MB-468 cell lines, GEF-H1, as well as PKD3 expression, was upregulated in oncospheres compared to the monolayer culture (2D). To validate a potential functional link between GEF-H1 and PKD3 in CSCs, we performed a transient GEF-H1 knockdown using two independent siRNAs prior to seeding of the cells into the primary oncosphere assay and then analyzed PKD3 activity. Remarkably, the depletion of GEF-H1 in MDA-MB-231 and MDA-MB-468 cells strongly reduced the activation loop phosphorylation of PKD3 and phosphorylation of its downstream target S6K1[19] in oncospheres (Figs. 3*g* and 3*h*, Supporting Information Fig. S2*l*). In line with these results,

we observed that the transient knockdown of PKD3 or GEF-H1 (Fig. 3*I*) significantly decreased SFE in the TNBC cell lines MDA-MB-231, MDA-MB-468, MDA-MB-436, BT-549 and HCC1806 but not in the luminal A breast cancer cell line MCF7 (Figs. 3*j* and 3*k*, Supporting Information Figs. S2*a*–S2*h*, *j*). Our data thus show that GEF-H1 activates PKD3 to promote stem cell maintenance.

PKD3 overexpression increases CSC-like properties

We next explored whether ectopic expression of PKD3 is sufficient to drive oncosphere formation in nontumorigenic breast epithelial MCF10A cells. Therefore, we generated a doxycycline (Dox)-inducible PKD3 (PKD3-EGFP) MCF10A cell line (Fig. 4*a*) and analyzed stem cell activity and marker gene expression. Indeed, the induction of PKD3-EGFP

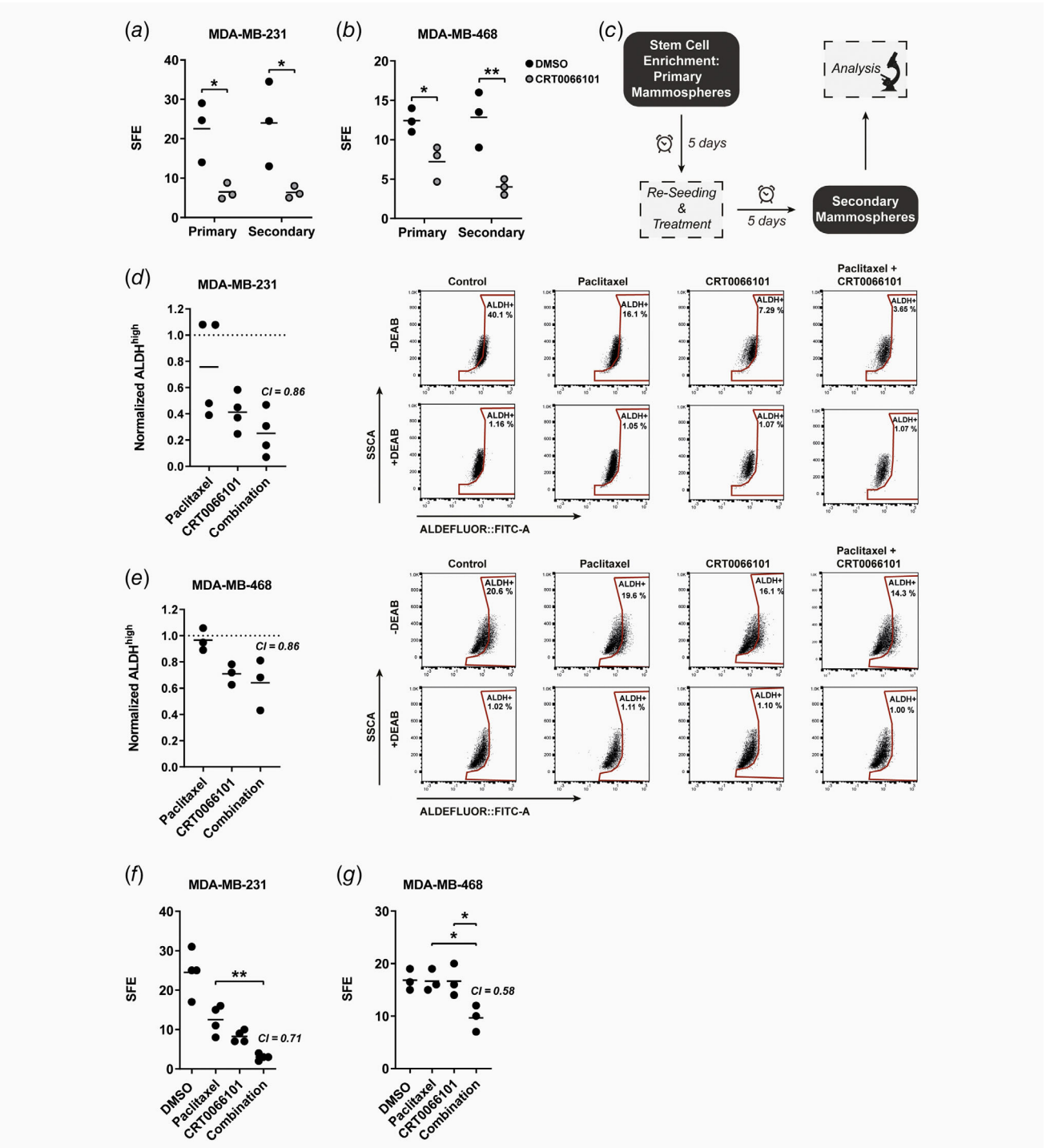

Figure 5. Legend on next page.

expression in MCF10A cells significantly increased SFE (Fig. 4*b*), without affecting the sphere area (Fig. 4*c*). Additionally, PKD3-EGFP increased the mRNA expression of stemness markers, such as SOX2 and OCT3/4[28,34] (Fig. 4*d*). To verify that GEF-H1 is required for PKD3-mediated stem cell maintenance also in the MCF10A model, we depleted GEF-H1 prior to inducing PKD3-EGFP expression and subjected the cells to a sphere formation assay. Strikingly, the depletion of GEF-H1 completely blocked the increase in sphere formation mediated by PKD3 (Figs. 4*e* and 4*f*), indicating that PKD3-mediated oncosphere formation is strictly dependent on GEF-H1.

Combined paclitaxel treatment and PKD3 inhibition synergistically decreases TNBC stem cell-mediated oncosphere and colony formation

Loss-of-function by stable or transient knockdown of PKD3 in TNBC cell lines revealed a crucial role for the kinase in CSC maintenance. We thus explored whether pharmacological inhibition of kinase activity using the selective pan-PKD inhibitor CRT0066101[17] would mimic the loss of PKD3 gene expression. First, we tested the efficacy of the inhibitor in oncosphere formation assays. Equally to PKD3 depletion, CRT0066101 treatment of MDA-MB-231, MDA-MB-468, MDA-MB-436 and BT-549 TNBC cells significantly reduced the number of primary and secondary oncospheres without affecting the respective sphere area (Figs. 5*a* and 5*b*, Supporting Information Figs. S3*a*–S3*d*). The chemotherapeutic paclitaxel is widely used in the clinical setting.[35] We therefore asked whether PKD inhibition sensitized TNBC cells to paclitaxel treatment. First, we tested the response behavior of MDA-MB-231 and MDA-MB-468 cells to the combination of paclitaxel and CRT0066101 in a 3D viability assay. Especially low, clinically relevant paclitaxel concentrations[36] as well as low micromolar CRT0066101 concentrations showed synergistic or additive effects (Supporting Information Figs. S3*e* and S3*f*). In line with these results, we further observed that shPKD3_1 cells were significantly more sensitive when treated with increasing concentrations of paclitaxel compared to shNon_CTRL cells (Supporting Information Fig. S3*g*). Next, we addressed potential synergistic effects of the combinatorial treatment on TNBC stem cells and analyzed ALDH activity as well as sphere-forming efficiency. We first performed a primary oncosphere formation assay to enrich for TNBC stem cells (Fig. 5*c*). These oncospheres were singularized, reseeded into a secondary oncosphere formation assay and immediately treated with either CRT0066101, paclitaxel or the combination of both. Both single and combination treatments reduced ALDH activity in MDA-MB-231 and MDA-MB-468 cells (Figs. 5*d* and 5*e*). Regarding SFE, the combination was highly synergistic in MDA-MB-231, MDA-MB-468, MDA-MB-436, BT-549 and HCC1806 TNBC cell lines (Figs. 5*f* and 5*g*, Supporting Information Fig. S4). Because clonogenic activity is a sensitive marker of undifferentiated CSCs,[37] we tested the combination treatment of CRT0066101 and paclitaxel in a colony formation assay. In line with our previous results, the combinatorial treatment synergistically decreased the clonogenic activity in MDA-MB-231, MDA-MB-468, MDA-MB-436 and BT-549 TNBC cells (Figs. 6*a* and 6*b*, Supporting Information Fig. S5). Thus, combining paclitaxel with CRT0066101 was superior to the single treatments and synergistically reduced the prevalence of CSCs in these TNBC cell lines.

The combination of CRT0066101 and paclitaxel is superior in decreasing tumor recurrence *in vivo*

Finally, we used an orthotopic xenograft mouse model to investigate the growth and recurrence of MDA-MB-231 tumors after treatment with paclitaxel, CRT0066101 or the combination of both. The cells were transplanted into SCID mice and allowed to form tumors with a size of ~100 mm^3. Compared to the control (vehicle only) CRT0066101 had only little effect on tumor growth. Accordingly, tumor-bearing mice belonging to the control and CRT0066101 groups had to be removed from the study shortly after the end of the treatment period. In contrast, paclitaxel caused an initial inhibition of tumor growth, which was further enhanced by CRT0066101. Upon therapy termination, paclitaxel-treated tumors displayed a strong regrowth. More importantly, in the posttreatment period, animals that had received the combination treatment showed a significant reduction in tumor regrowth compared to paclitaxel treated animals (Figs. 6*c* and 6*d*), providing support for the superior targeting of

Figure 5. The combination of paclitaxel and CRT0066101 synergistically reduces sphere formation *in vitro*. (*a*, *b*) Counting of primary and secondary oncospheres of (*a*) MDA-MB-231 and (*b*) MDA-MB-468 cells. Cells were treated with 1 μM CRT0066101 directly after seeding into the respective oncosphere assay. Data are presented as mean sphere formation efficiency (SFE), $n = 3$. Statistical comparison by one-way ANOVA and Bonferroni test. (*c*) Workflow of paclitaxel and CRT0066101 oncosphere treatment. (*d*, *e*) *Left panel*: Flow cytometry-based stemness analysis of (*d*) MDA-MB-231 or (*e*) MDA-MB-468 cells *via* ALDEFLUOR™. Directly after seeding into the secondary oncosphere assay, cells were treated with paclitaxel (5 nM) or CRT0066101 (MDA-MB-231: 1 μM; MDA-MB-468: 0.5 μM), or in combination. DMSO served as control. Data is presented as mean $ALDH^{high}$ population normalized to DMSO control, $n = 3–4$. Statistical comparison by one-way ANOVA and Bonferroni test. Combination index (CI) values were calculated *via* Webb's fractional product method using the respective mean of % $ALDH^{high}$ populations. CI < 1 indicates synergism. *Right panels*: Dot plot of ALDEFLUOR measurements. DEAB-treated samples served as internal control. (*f*, *g*) Counting of secondary oncospheres of (*f*) MDA-MB-231 and (*g*) MDA-MB-468 cells. Directly after seeding into the secondary oncosphere assay, cells were treated with paclitaxel (5 nM) or CRT0066101 (MDA-MB-231: 1 μM; MDA-MB-468: 0.5 μM), or in combination. DMSO served as control. Data are presented as mean sphere formation efficiency (SFE), $n = 3–4$. Statistical comparison by one-way ANOVA and Bonferroni-test. Combination index (CI) values were calculated using Webb's fractional product method. CI < 1 indicates synergism. [Color figure can be viewed at wileyonlinelibrary.com]

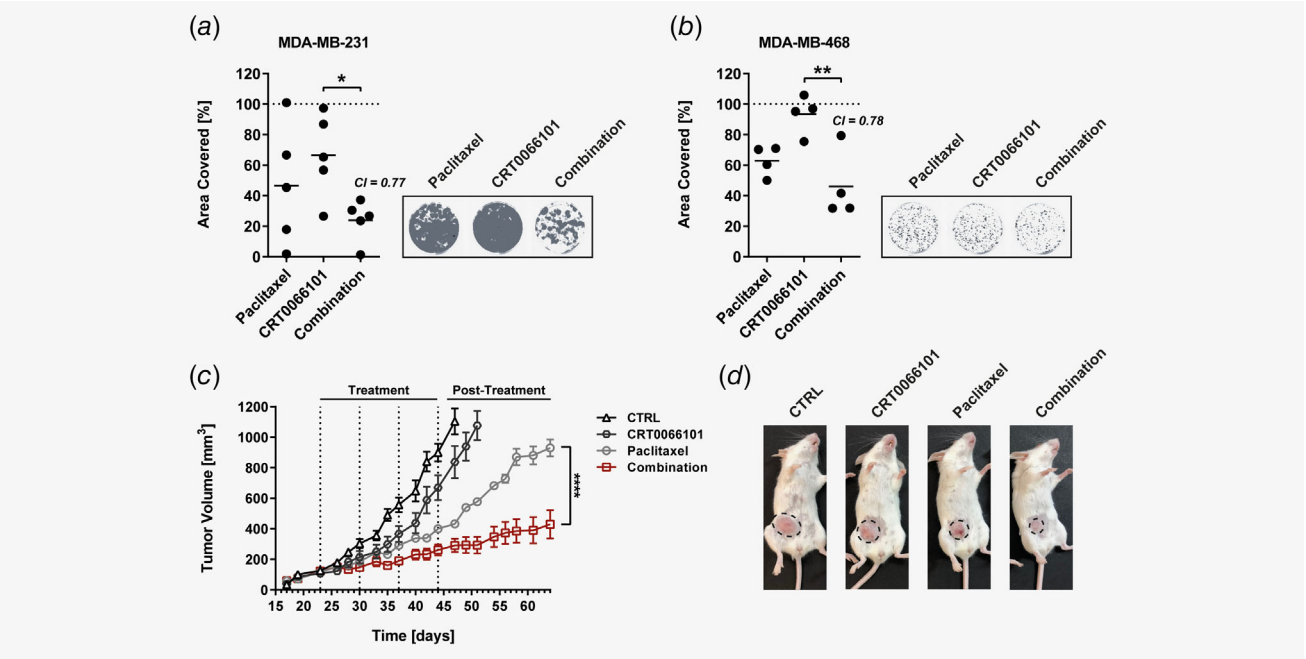

Figure 6. The combination of paclitaxel and CRT0066101 synergistically reduces colony formation *in vitro* as well as tumor recurrence *in vivo*. (*a*,*b*) *Left panels*: colony formation of (*a*) MDA-MB-231 and (*b*) MDA-MB-468 cells. 24 hr after seeding into six-well culture dishes, MDA-MB-231 and MDA-MB-468 cells were treated for 48 hr with paclitaxel (1 nM) or CRT0066101 (MDA-MB-231: 1 μM; MDA-MB-468: 0.1 μM), or the combination of both. DMSO served as control. Afterward, cells were further cultured for 2 weeks and analyzed using the Odyssey imaging system. Data are presented as mean area covered. DMSO control was set to 100%, $n = 4–5$. Statistical comparison by one-way ANOVA and Bonferroni test. Combination index (CI) values were calculated using Webb's fractional product method. CI < 1 indicates synergism. *Right panels*: Representative pictures of the respective colony formation assays. (*c*) Eight-week-old female SCID mice were injected with 2×10^6 MDA-MB-231 cells into the right fat pad of the fourth nipple. After the tumors had reached 100 mm^3 mice were treated with either CRT0066101, paclitaxel or the combination of both. The combination of the respective carriers served as control. Data are presented as tumor volume (mm^3), mean ± SEM, $n = 7$. Statistical comparison by two-way ANOVA and Bonferroni test. (*d*) Representative pictures of animals from the respective treatment groups. Tumors are indicated by dotted circles.

drug-resistant cancer cell subpopulations by paclitaxel plus CRT0066101.

Discussion

PKD3 has been associated with TNBC progression[17,19] but so far, a specific role for PKD3 in CSC stemness has not been described. In our study, we have defined a critical role for PKD3 in the maintenance and propagation of TNBC stem cells *in vitro* and *in vivo*. The PKD inhibitor CRT0066101 demonstrated strong efficacy in eliminating TNBC stem cells *in vitro*. More importantly, CRT0066101 synergistically increased the response to paclitaxel *in vitro* and *in vivo*. These findings are of high clinical relevance as taxanes have shown to increase the TNBC stem cell population.[6,7,38] Thus, inhibiting PKD3 in combination with paclitaxel has a dual effect by targeting differentiated cancer cells and at the same time eradicating the cell population responsible for chemoresistance and tumor recurrence.

The role of PKD3 in cancer stemness was specific for TNBC cell lines as in luminal A MCF7 cells with only marginal PKD3 expression depletion of the kinase did not affect oncosphere formation (Supporting Information Fig. S2*h*). Our findings further support the postulated isoform switch from PKD1 to PKD3 in breast tumor progression. While PKD1 is a negative regulator of cell motility and invasion and contributes to the maintenance of the epithelial phenotype of breast cells, PKD3 drives cell proliferation and invasion[17] and, as shown in our study, CSC maintenance.

Taxanes were shown to increase the CSC population in patients with invasive breast cancer.[6,7,9] Moreover, paclitaxel increased the ALDH-positive population in MDA-MB-231 cells by enhancing SOX2, ABCG2 and TWIST1 expression, unraveling an interconnected pluripotency–chemoresistance–EMT (epithelial to mesenchymal transition) axis.[8] EMT is linked to breast CSC regulation, and exposing TNBC cells to the EMT inducer transforming growth factor-beta (TGF-β) increased oncosphere formation and the $CD44^+/CD24^-$ stem cell signature.[39] Interestingly, PKD3 has also been connected with EMT, as treating MDA-MB-231 cells with CRT0066101 reduced the expression of the EMT transcription factor SNAI1.[40] Strikingly, PKD3 depletion in MDA-MB-231 cells decreased SOX2, ABCG2, SLUG and SNAI1 expression (Fig. 1*e*, Supporting Information Figs. S2*k* and S2*o*) and increased CDH1 expression in BT549 cells (Supporting Information Fig. S2*p*). PKD3

inhibition thus likely counteracts the paclitaxel-induced upregulation of EMT genes. Breaking up the pluripotency–chemoresistance–EMT axis might contribute to the strong response to combined CRT0066101 and paclitaxel treatment *in vivo*.

We further identified GEF-H1 to be upstream of PKD3 activity in oncosphere formation, in support of the proposed contribution of GEF-H1/Rho signaling to breast cancer metastasis.[41] However, how does GEF-H1/PKD3 signaling contribute to the maintenance of TNBC stem cells? Recently, we showed that a GEF-H1-RhoA-PLCε-PKD pathway regulates the fission of exocytic vesicles at the Golgi complex.[33] The changes in surface protein expression upon PKD3 depletion could thus stem from deregulated exocytosis. Various secreted factors derived from the bulk tumor and CSC population, acting in paracrine and autocrine manners, are required for the CSC survival. For example, in basal-like breast cancer, the mesenchymal-like tumor cells were reported to produce WNT2, CXCL12 and IL6, which drive the self-renewal of the CSCs.[42] Furthermore, TGF-β together with autocrine canonical and noncanonical WNT signaling controls migratory and self-renewal ability of breast CSCs by promoting the expression of EMT-associated transcription factors.[43] By promoting the secretion of paracrine and/or autocrine survival factors PKD3 signaling might positively regulate the expression of EMT-associated transcription factors to maintain the CSC state. In support of our hypothesis, Zeng *et al.*[44] reported that the mesenchymal stem cell marker CD146 promotes EMT through RhoA-induced upregulation of SLUG thereby contributing to the maintenance of CSC-like cells in breast cancer. Our data further indicate that PKD3 depletion reduces YAP/TAZ signaling (Supporting Information Fig. S1*o*), congruent with the reported regulation of YAP/TAZ signaling by PKD in pancreatic cancer cells.[45] EMT induces and requires YAP/TAZ for triggering breast cancer stemness and metastasis[32] and *vice versa*, YAP/TAZ are active inducers of EMT.[46,47] This suggests that several positive and negative feedback loops are in place to sustain the maintenance of CSCs.

TNBC patients have a high probability of tumor recurrence within the first 5 years after the end of treatment, which is largely driven by CSC activity.[30,48,49] The development of new therapeutic strategies targeting TNBC stem cells has thus been intensified over the last years.[50] For example, the kinase inhibitor Dasatinib and TGF-β pathway inhibition, respectively, were shown to enhance the responsiveness to paclitaxel treatment in preclinical models of TNBC.[51] Thus, these studies and our results demonstrate that combining paclitaxel with therapeutic antibodies or small molecule inhibitors such as CRT0066101 has great clinical potential by targeting more effectively the TNBC bulk tumor and stem cell populations.

Acknowledgements

This project was supported by the Deutsche Krebshilfe (grant 70111941 to M.A.O. and A. H). P.S. was supported by the NIH grants CA184527 and CA200572.

References

1. Perou CM, Sorlie T, Eisen MB, et al. Molecular portraits of human breast tumours. *Nature* 2000; 406:747–52.
2. Liedtke C, Mazouni C, Hess KR, et al. Response to neoadjuvant therapy and long-term survival in patients with triple-negative breast cancer. *J Clin Oncol* 2008;26:1275–81.
3. Smid M, Wang Y, Zhang Y, et al. Subtypes of breast cancer show preferential site of relapse. *Cancer Res* 2008;68:3108–14.
4. Foulkes WD, Smith IE, Reis-Filho JS. Triple-negative breast cancer. *N Engl J Med* 2010;363:1938–48.
5. von Minckwitz G, Schneeweiss A, Loibl S, et al. Neoadjuvant carboplatin in patients with triple-negative and HER2-positive early breast cancer (GeparSixto; GBG 66): a randomised phase 2 trial. *Lancet Oncol* 2014;15:747–56.
6. Creighton CJ, Li X, Landis M, et al. Residual breast cancers after conventional therapy display mesenchymal as well as tumor-initiating features. *Proc Natl Acad Sci USA* 2009;106:13820–5.
7. Li X, Lewis MT, Huang J, et al. Intrinsic resistance of tumorigenic breast cancer cells to chemotherapy. *J Natl Cancer Inst* 2008;100:672–9.
8. Mukherjee P, Gupta A, Chattopadhyay D, et al. Modulation of SOX2 expression delineates an end-point for paclitaxel-effectiveness in breast cancer stem cells. *Sci Rep* 2017;7:9170.
9. Lin Y, Zhong Y, Guan H, et al. CD44+/CD24− phenotype contributes to malignant relapse following surgical resection and chemotherapy in patients with invasive ductal carcinoma. *J Exp Clin Cancer Res* 2012;31:59.
10. Adamczyk A, Niemiec JA, Ambicka A, et al. CD44/CD24 as potential prognostic markers in node-positive invasive ductal breast cancer patients treated with adjuvant chemotherapy. *J Mol Histol* 2014;45:35–45.
11. Ma F, Li H, Li Y, et al. Aldehyde dehydrogenase 1 (ALDH1) expression is an independent prognostic factor in triple negative breast cancer (TNBC). *Medicine (Baltimore)* 2017;96:e6561.
12. Abraham BK, Fritz P, McClellan M, et al. Prevalence of CD44+/CD24−/low cells in breast cancer may not be associated with clinical outcome but may favor distant metastasis. *Clin Cancer Res* 2005;11:1154–9.
13. Al-Hajj M, Wicha MS, Benito-Hernandez A, et al. Prospective identification of tumorigenic breast cancer cells. *Proc Natl Acad Sci USA* 2003;100: 3983–8.
14. Fu Y, Rubin CS. Protein kinase D: coupling extracellular stimuli to the regulation of cell physiology. *EMBO Rep* 2011;12:785–96.
15. Olayioye MA, Barisic S, Hausser A. Multi-level control of Actin dynamics by protein kinase D. *Cell Signal* 2013;25:1739–47.
16. Borges S, Doppler H, Perez EA, et al. Pharmacologic reversion of epigenetic silencing of the PRKD1 promoter blocks breast tumor cell invasion and metastasis. *Breast Cancer Res* 2013; 15:R66.
17. Borges S, Perez EA, Thompson EA, et al. Effective targeting of Estrogen receptor-negative breast cancers with the protein kinase D inhibitor CRT0066101. *Mol Cancer Ther* 2015;14:1306–16.
18. Hao Q, McKenzie R, Gan H, et al. Protein kinases D2 and D3 are novel growth regulators in HCC1806 triple-negative breast cancer cells. *Anticancer Res* 2013;33:393–9.
19. Huck B, Duss S, Hausser A, et al. Elevated protein kinase D3 (PKD3) expression supports proliferation of triple-negative breast cancer cells and contributes to mTORC1-S6K1 pathway activation. *J Biol Chem* 2014;289:3138–47.
20. Huck B, Kemkemer R, Franz-Wachtel M, et al. GIT1 phosphorylation on serine 46 by PKD3 regulates paxillin trafficking and cellular protrusive activity. *J Biol Chem* 2012;287:34604–13.
21. Hu Y, Smyth GK. ELDA: extreme limiting dilution analysis for comparing depleted and enriched populations in stem cell and other assays. *J Immunol Methods* 2009;347:70–8.
22. Bossard C, Bresson D, Polishchuk RS, et al. Dimeric PKD regulates membrane fission to form transport carriers at the TGN. *J Cell Biol* 2007; 179:1123–31.
23. Dubrovska A, Hartung A, Bouchez LC, et al. CXCR4 activation maintains a stem cell population in tamoxifen-resistant breast cancer cells

through AhR signalling. *Br J Cancer* 2012;107:43–52.
24. Vaillant F, Asselin-Labat ML, Shackleton M, et al. The mammary progenitor marker CD61/beta3 integrin identifies cancer stem cells in mouse models of mammary tumorigenesis. *Cancer Res* 2008;68:7711–7.
25. Glinka Y, Mohammed N, Subramaniam V, et al. Neuropilin-1 is expressed by breast cancer stem-like cells and is linked to NF-kappaB activation and tumor sphere formation. *Biochem Biophys Res Commun* 2012;425:775–80.
26. Yen WC, Fischer MM, Axelrod F, et al. Targeting notch signaling with a Notch2/Notch3 antagonist (tarextumab) inhibits tumor growth and decreases tumor-initiating cell frequency. *Clin Cancer Res* 2015;21:2084–95.
27. Harrison H, Farnie G, Howell SJ, et al. Regulation of breast cancer stem cell activity by signaling through the Notch4 receptor. *Cancer Res* 2010;70:709–18.
28. Leis O, Eguiara A, Lopez-Arribillaga E, et al. Sox2 expression in breast tumours and activation in breast cancer stem cells. *Oncogene* 2012;31:1354–65.
29. Iriondo O, Rabano M, Domenici G, et al. Distinct breast cancer stem/progenitor cell populations require either HIF1alpha or loss of PHD3 to expand under hypoxic conditions. *Oncotarget* 2015;6:31721–39.
30. Ginestier C, Hur MH, Charafe-Jauffret E, et al. ALDH1 is a marker of normal and malignant human mammary stem cells and a predictor of poor clinical outcome. *Cell Stem Cell* 2007;1:555–67.
31. Cioce M, Gherardi S, Viglietto G, et al. Mammosphere-forming cells from breast cancer cell lines as a tool for the identification of CSC-like- and early progenitor-targeting drugs. *Cell Cycle* 2010;9:2878–87.
32. Cordenonsi M, Zanconato F, Azzolin L, et al. The hippo transducer TAZ confers cancer stem cell-related traits on breast cancer cells. *Cell* 2011;147:759–72.
33. Eisler SA, Curado F, Link G, et al. A rho signaling network links microtubules to PKD controlled carrier transport to focal adhesions. *Elife* 2018;7:e35907.
34. Hu T, Liu S, Breiter DR, et al. Octamer 4 small interfering RNA results in cancer stem cell-like cell apoptosis. *Cancer Res* 2008;68:6533–40.
35. McAndrew N, DeMichele A. Neoadjuvant chemotherapy considerations in triple-negative breast cancer. *J Target Ther Cancer* 2018;7:52–69.
36. Zasadil LM, Andersen KA, Yeum D, et al. Cytotoxicity of paclitaxel in breast cancer is due to chromosome missegregation on multipolar spindles. *Sci Transl Med* 2014;6:229ra43.
37. Rajendran V, Jain MV. In vitro tumorigenic assay: Colony forming assay for cancer stem cells. *Methods Mol Biol* 2018;1692:89–95.
38. Gomez-Miragaya J, Palafox M, Pare L, et al. Resistance to Taxanes in triple-negative breast cancer associates with the dynamics of a CD49f+ tumor-initiating population. *Stem Cell Rep* 2017;8:1392–407.
39. Mani SA, Guo W, Liao MJ, et al. The epithelial-mesenchymal transition generates cells with properties of stem cells. *Cell* 2008;133:704–15.
40. Durand N, Borges S, Storz P. Protein kinase D enzymes as regulators of EMT and cancer cell invasion. *J Clin Forensic Med* 2016;5:E20.
41. Liao YC, Ruan JW, Lua I, et al. Overexpressed hPTTG1 promotes breast cancer cell invasion and metastasis by regulating GEF-H1/RhoA signalling. *Oncogene* 2012;31:3086–97.
42. Zhang M, Tsimelzon A, Chang CH, et al. Intratumoral heterogeneity in a Trp53-null mouse model of human breast cancer. *Cancer Discov* 2015;5:520–33.
43. Scheel C, Eaton EN, Li SH, et al. Paracrine and autocrine signals induce and maintain mesenchymal and stem cell states in the breast. *Cell* 2011;145:926–40.
44. Zeng Q, Li W, Lu D, et al. CD146, an epithelial-mesenchymal transition inducer, is associated with triple-negative breast cancer. *Proc Natl Acad Sci USA* 2012;109:1127–32.
45. Wang J, Sinnett-Smith J, Stevens JV, et al. Biphasic regulation of yes-associated protein (YAP) cellular localization, phosphorylation, and activity by G protein-coupled receptor agonists in intestinal epithelial cells: a novel role for protein kinase D (PKD). *J Biol Chem* 2016;291:17988–8005.
46. Shao D, Zhai P, Del Re DP, et al. A functional interaction between hippo-YAP signalling and FoxO1 mediates the oxidative stress response. *Nat Commun* 2014;5:3315.
47. Zhao B, Wei X, Li W, et al. Inactivation of YAP oncoprotein by the hippo pathway is involved in cell contact inhibition and tissue growth control. *Genes Dev* 2007;21:2747–61.
48. Stratford AL, Reipas K, Maxwell C, et al. Targeting tumour-initiating cells to improve the cure rates for triple-negative breast cancer. *Expert Rev Mol Med* 2010;12:e22.
49. Rangel MC, Bertolette D, Castro NP, et al. Developmental signaling pathways regulating mammary stem cells and contributing to the etiology of triple-negative breast cancer. *Breast Cancer Res Treat* 2016;156:211–26.
50. Tian J, Raffa FA, Dai M, et al. Dasatinib sensitises triple negative breast cancer cells to chemotherapy by targeting breast cancer stem cells. *Br J Cancer* 2018;119:1495–507.
51. Bhola NE, Balko JM, Dugger TC, et al. TGF-beta inhibition enhances chemotherapy action against triple-negative breast cancer. *J Clin Invest* 2013;123:1348–58.